Molecular Structure, Vibrational Spectra, and Hydrogen Bonding of the Ionic Liquid 1-Ethyl-3-methyl-1*H*-imidazolium Tetrafluoroborate

by **Sergey A. Katsyuba***[a]), **Paul J. Dyson**[b]), **Elena E. Vandyukova**[a]), **Alla V. Chernova**[a]), and **Ana Vidiš**[b])

[a]) A. E. Arbuzov Institute of Organic and Physical Chemistry, Kazan Scientific Centre of the Russian Academy of Sciences, Arbuzov str. 8, 420088 Kazan, Russia
(e-mail: katsyuba@iopc.knc.ru; fax: +7-8432732253; tel: +7-8432727483)
[b]) Institut des Sciences et Ingénierie Chimiques, Ecole Polytechnique Fédérale de Lausanne, (EPFL) BCH, CH-1015 Lausanne

The IR and *Raman* spectra and conformations of the ionic liquid 1-ethyl-3-methyl-1*H*-imidazolium tetrafluoroborate, [EMIM][BF_4] (**6**), were analyzed within the framework of scaled quantum mechanics (SQM). It was shown that SQM successfully reproduced the spectra of the ionic liquid. The computations revealed that normal modes of the $EMIM^+ \cdot BF_4^-$ ion pair closely resemble those of the isolated ions $EMIM^+$ and BF_4^-, except for the antisymmetric BF stretching vibrations of the anion, and the out-of-plane and stretching vibrations of the H–C(2) moiety of the cation. The most plausible explanation for the pronounced changes of the latter vibrations upon ion-pair formation is the H-bonding between H–C(2) and BF_4^-. However, these weak H-bonds are of minor importance compared with the *Coulomb* interactions between the ions that keep them closely associated even in dilute CD_2Cl_2 solutions. According to the 'gas-phase' computations, in these associates, the BF_4^- anion is positioned over the imidazolium ring of the $EMIM^+$ cation and has short contacts not only with the H–C(2) of the latter, but also with a proton of the Me–N(3) group.

Introduction. – Ionic liquids (or, more specifically, room-temperature ionic liquids (RTIL)) are salts exhibiting liquidity at or below a given temperature, often conveniently taken to be 100°, and contain organic cations rather than inorganic cations [1]. The vast majority of work published to date on RTILs relates to systems based on *N*-alkylpyridinium and 1-alkyl-3-methyl-1*H*-imidazolium cations, originally combined with chloroaluminate(III) anions. The chloroaluminate liquids proved to be unstable in air, but this problem was overcome through the use of alternative anions such as BF_4^-, PF_6^-, *etc.* These apparently stable RTILs attract interest as nonvolatile, environmentally friendly solvents.

An important aspect of RTILs is the nature of the interactions among the ions present and questions of particular interest include the following. Is there ion-pair formation in the melt? Are there specific points on the 1-ethyl-3-methyl-1*H*-imidazolium ($EMIM^+$) cation where interactions with counterions occur? In a crystallographic and IR study [2] of [EMIM]Cl (**1**) the chloride was observed to be located in H-bond positions (H–C(2), H–C(4), and H–C(5)) characteristic of C–H $\cdots Cl^-$ interactions. The most obvious feature of the IR spectra of both the solid compound and the melts is the presence of the so called 'Cl^- interaction band' [3] at *ca.* 3050 cm^{-1}, which is assigned to stretching vibrations of H–C(2), H–C(4), and H–C(5) H-bonded to the chloride anion. Similar Br^- and I^- interaction bands are also found [4] between 3050 and 3080 cm^{-1} in the spectra of [EMIM]Br (**2**) and [EMIM]I

(**3**). According to X-ray data [4], the local structure around the EMIM cation is similar to that observed for **1**. Namely, each cation is H-bonded *via* H−C(2), H−C(4), and H−C(5) bonds to three anions, lying approximately in the plane of the ring. *Ab initio* HF and MP2 computations [5] for **1**–**3** demonstrate that these three positions of the halogen ion correspond to local minima on the potential-energy surface of the isolated molecules. Of these three local minima, the one with the halogen ion positioned to interact with the most acidic proton, *viz.* H−C(2), generally have the lowest energy. The global minimum corresponds to the halogen ion positioned over the ring in a close proximity to H−C(2). Molecular-dynamic simulations [6] and neutron-diffraction studies [1] of the melt of **1** also locate Cl^- in both the plane of the ring and in out-of-plane positions.

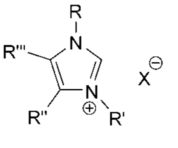

1 R = Et, R' = Me, R'' = R''' = H, X = Cl
2 R = Et, R' = Me, R'' = R''' = H, X = Br
3 R = Et, R' = Me, R'' = R''' = H, X = I
4 R = Bu, R' = Me, R'' = R''' = H, X = BF_4
5 R = R' = ^{i}Pr, R'' = R''' = Me, X = BF_4
6 R = Et, R' = Me, R'' = R''' = H, X = BF_4
7 R = Et, R' = Me, R'' = R''' = H, X = PF_6
8 R = Bu, R' = Me, R'' = R''' = H, X = PF_6

Compared to the halides that have been thoroughly studied, little is known about the ionic structure of imidazolium tetrafluoroborates and their capacity for H-bonding. The IR spectrum of 1-butyl-3-methyl-1*H*-imidazolium tetrafluoroborate (**4**) [7] exhibits two aromatic C−H stretching bands at 3165 and 3122 cm^{-1}. The latter is ascribed [7], by analogy with 'haloid interaction bands', to H-bonding between C−H and BF_4^-. According to X-ray data [8] obtained on a single crystal of 1,3-diisopropyl-4,5-dimethyl-1*H*-imidazolium tetrafluoroborate (**5**), the BF_4^- anion is localized in the plane of the ring and in moderately close contact with H−C(2). At the same time, the C(2)−H···F distance is *ca.* 0.1 Å longer than the distance between another F-atom of the tetrafluoroborate anion and a proton of the ^{i}Pr moiety of the second neighboring cation. So, it is not quite clear whether H-bonding is present in 1,3-dialkyl-1*H*-imidazolium tetrafluoroborates or whether the short contacts have another origin.

Vibrational spectroscopy is a versatile tool in probing H-bonding of both liquid and solid compounds or their solutions. In this paper, we present results from IR and *Raman* spectroscopic experiments as well as *ab initio* HF and density-functional-theory (DFT) [9] calculations of the structure and vibrational modes of [EMIM][BF_4] (**6**). As will be discussed, the computations are used to assign the IR and *Raman* bands and provide information on the structures of the isolated ions.

Experimental. – The title compound **6** was synthesized by using a previously described procedure [10]. The solvent CD_2Cl_2 was purchased from *Armar AG* and used without further purification. All soln. preparations were carried out in a glove box with exclusion of moisture. IR Spectra: FT-IR spectrometers *Bruker Vector 22* in the 400–4000 cm^{-1} range at a resolution of 1 cm^{-1} and *Bruker IFS 113v* in the 200–650 cm^{-1} range at a resolution of 1 cm^{-1}; liquid samples as thin films between KBr plates; CD_2Cl_2 solns. in 0.27-mm NaCl cells, concentrations *ca.* 10^{-1} M. *Raman* spectra: *Coderg PHO-82* spectrometer with a double monochromator; a He−Ne laser (LG-36A, λ 632.8 nm, power 30 mW); samples in standard glass capillaries.

Computations. – All *ab initio* calculations were done by using the Gaussian-98 suite of programs [11]. For DFT, *Becke*'s three-parameter exchange functional [12] was used in combination with the *Lee–Yang–Parr* correlation functional [13] (B3LYP) and standard 6-31G* and 6-31 + G* basis sets. All stationary points were characterized as minima by analysis of the Hessian matrices. The calculated force fields were transformed to internal coordinates, and the scaling procedure was applied with the use of the program described in [14]. The reason being that though DFT produces surprisingly accurate vibrational frequencies, even these computations show systematic errors mainly due to limited basis sets, harmonic approximation, and remaining deficiencies in describing electron correlation. Transferable scaling factors (SF) compensate for most of these errors [15]. It has been demonstrated earlier that the scaled quantum-mechanics (SQM) method allows *a priori* quantitative prediction of the IR and *Raman* spectra of organic molecules, including the atoms H, C, O, N, S, P, and Cl [16–18]. Since SQM has not yet been applied to systems containing B- and F-atoms, we derived SF for stretching and bending force constants of BF_4^- from a training set of two molecules: BF_3 and $BFCl_2$. Their transferability was tested by comparison of SQM-predicted vibrational frequencies of BF_2Cl with the corresponding experimental values¹). These transferable SF are summarized in *Table 1* together with all other SF employed in this work.

Table 1. *Scaling Factors for the Force Fields of* **6** *and* **7**

Scaling factor		Value
stretch	CC	0.9207 ᵃ)
stretch	CH (arom.)	0.915 ᵇ)
stretch	CH (aliph.)	0.889 ᵇ)
stretch	CN	0.9207 ᵃ)
stretch	BF	1.0000 ᶜ)
bend	CNC	1.0144 ᵃ)
bend	CCC	1.0144 ᵃ)
bend	FBF	1.0144 ᶜ)
bend	CCH	0.950 ᵃ)
bend	HCH	0.9016 ᵃ)
torsion	all	0.9523 ᵃ)
out of plane	ring-H, ring-C	0.976 ᵃ)

ᵃ) Ref. [16]. ᵇ) Ref. [17]. ᶜ) This work (see text).

Results and Discussion. – Calculations were initially used to optimize all the possible rotamers of the isolated 1-ethyl-3-methyl-1*H*-imidazolium cation, $EMIM^+$. The only minimum on the potential-energy surface corresponded to the conformer, shown in *Figs. 1–3*, at B3LYP level. The conformation as well as calculated structural parameters of the imidazolium ring are in good agreement with the X-ray data available for the EMIM halides **2** and **3** [4] and hexafluorophosphate **7** [19] (see *Table 2*). HF Computations predicted also another less stable conformation with the Et moiety lying in the plane of the ring [5], but this minimum disappeared when the $EMIM^+ \cdot BF_4^-$ system was optimized. Initiation of the $EMIM^+ \cdot BF_4^-$ ion-pair computations was conducted by placing the anion above and below the imidazolium ring, also at the different sides of the ring, including possible H-bond positions near H–C(2), H–C(4), and H–C(5). Only one final structure was found for each method after optimization (*Figs. 1–3*), irrespective of the starting point. Unlike the chloride systems, where the chloride was found in the plane of the ring [2][5], BF_4^- is positioned over the ring and has short contacts not only with H–C(2), but also with a proton of the Me group. Similar results were obtained by several authors [20][21] during the course

---

¹) The detailed tables of calculated and experimental frequencies of BF_3, BF_2Cl, and $BFCl_2$, together with the assignments, based on computed potential-energy distributions, and complete references are placed in supplementary material available on request from the authors.

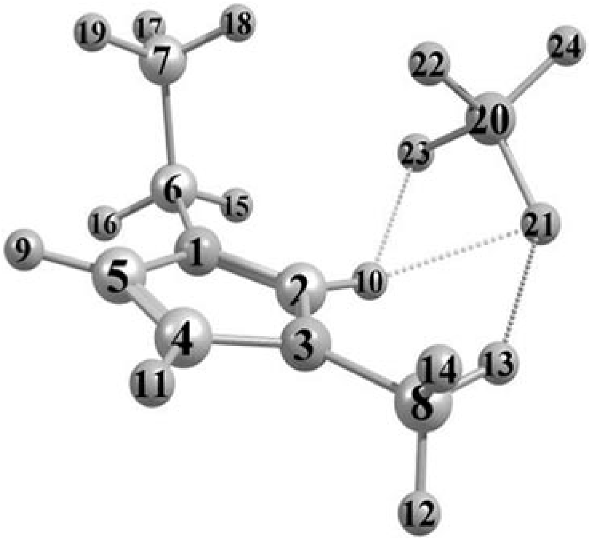

Fig. 1. *HF/6-31G*-Calculated molecular structure of [EMIM][BF_4]* (**6**). Arbitrary numbering, F···H distances [Å]: F(21)–H(13) 2.3019, F(21)–H(10) 2.1330, F(23)–H(10) 2.1162.

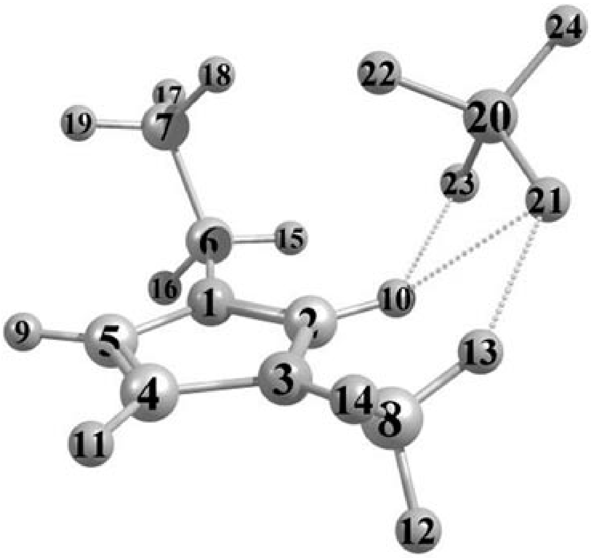

Fig. 2. *B3LYP/6-31G*-Calculated molecular structure of [EMIM][BF_4]* (**6**). Arbitrary numbering. F···H distances [Å]: F(21)–H(13) 2.1661, F(21)–H(10) 2.1587, F(23)–H(10) 1.9360.

of *ab initio* structure optimization of 1-butyl-3-methyl-1*H*-imidazolium hexafluorophosphate (**8**). The computations agree well with the single-crystal X-ray structure of **7** [19]. Probably, this out-of-plane anion position near the most acidic proton H–C(2) is

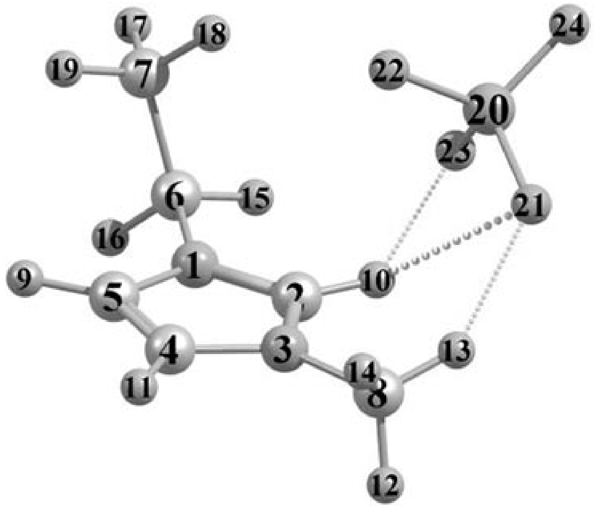

Fig. 3. *B3LYP/6–31 + G*-Calculated molecular structure of [EMIM][BF$_4$]* (**6**). Arbitrary numbering. F···H distances [Å]: F(21)–H(13) 2.2296, F(21)–H(10) 2.2861, F(23)–H(10) 2.0298.

Table 2. *Results Obtained from the B3LYP/6-31G* Geometry Optimization* (bond lengths/Å; angles/°) *for EMIM$^+$ in Comparison with X-Ray Data of Different EMIM Salts.* For numbering scheme, see *Fig. 1.*

Bonds	B3LYP/6-31G*	X-ray			Angles	B3LYP/6-31G*	X-ray		
	EMIM$^+$	**2** [4]	**3** [4]	**7** [19]		EMIM$^+$	**2** [4]	**3** [4]	**7** [19]
N(1)–C(5)	1.385	1.376	1.374	1.356	N(1)–C(5)–C(4)	107.2	106.5	107.4	107.5
C(4)–C(5)	1.363	1.352	1.322	1.330	N(3)–C(4)–C(5)	106.9	107.4	107.7	107. 8
N(3)–C(4)	1.385	1.367	1.368	1.366	C(2)–N(1)–C(5)	108.5	108.8	107.7	107.9
C(2)–N(1)	1.335	1.327	1.324	1.324	C(2)–N(3)–C(8)	123.9	125.0	123.8	125.6
N(3)–C(8)	1.467	1.449	1.462	1.463	C(6)–N(1)–C(5)	127.0	125.3	126.4	126.5
N(1)–C(6)	1.480	1.489	1.475	1.485	C(7)–C(6)–N(1)	111.3	111.6	111.5	111.5
C(6)–C(7)	1.527	1.472	1.475	1.505					

a common feature of imidazolium salts containing large and weakly coordinating perfluoro anions. To gain insight into the mutual orientation of the anions and cations in liquid **6** and in solutions, IR and *Raman* spectroscopic studies were undertaken.

The IR spectra of the ionic liquid **6** and of CD$_2$Cl$_2$ solutions of **6** obtained at 25° are shown in *Fig. 4*, and the band positions are listed in *Table 3* together with experimental *Raman* line positions and assignments based on the present SQM computations. The latter demonstrate a good general agreement between the calculated and the experimental wavenumbers of the fundamentals.

According to *Table 3*, the spectra of **6** may be qualitatively analyzed in terms of the vibrational modes of the BF$_4^-$ anion and those of the EMIM$^+$ cation. In so far as these modes practically do not mix, they retain their individuality. Consequently, it is possible to compare the vibrational frequencies of the separated ions (see *Tables 4* and *5*) and the ion pair EMIM$^+$ · BF$_4^-$ (*Table 3*). Our computations demonstrate that the ion-pair formation strongly influences three antisymmetrical BF stretching vibrations of the anion, and out-of-plane and stretching vibrations of the H–C(2) moiety of the cation

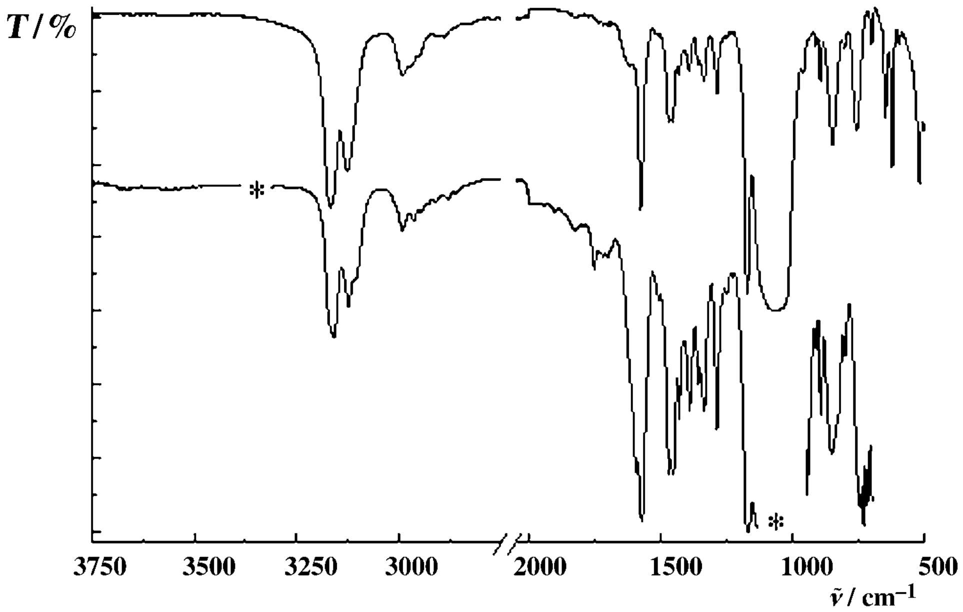

Fig. 4. *IR Spectra of liquid [EMIM][BF$_4$]* (**6**) *(top) and [EMIM][BF$_4$]* (**6**) *solution in CD$_2$Cl$_2$* (bottom). Regions of strong absorption of CD$_2$Cl$_2$ are marked with asterisks.

(*Tables 3–5*). All other fundamentals are almost completely transferable between the individual ions and the ion pair.

From *Tables 3* and *4* it is apparent that all three CH stretching modes of the imidazolium ring are practically degenerate in the absence of the BF$_4^-$ anion, and as a result, the only $\tilde{\nu}$(CH) band (*ca.* 3170 cm^{-1}) should be observed in the IR spectra for the isolated cation. The red shift of the $\tilde{\nu}$(H–C(2)) band, caused by the interaction with the anion, removes the degeneracy, and the second band at *ca.* 3130 cm^{-1} arises in the spectrum of liquid **6**. By analogy with 'haloid interaction bands' [3], this lower-wavelength band may be ascribed to H-bonding between the cation and the anion. According to computations, the BF$_4^-$ ··· H–C(2) short contact induces not only a red shift of the $\tilde{\nu}$(H–C(2)) band, but also a substantial growth of its IR intensity. The latter is regarded as the most reliable marker of H-bond formation [22], though this effect is overestimated by B3LYP computations. And, at last, the dramatic increase of the H–C(2) out-of-plane wavenumber of EMIM$^+$ during the course of the ion-pair formation (*cf. Tables 3* and *4*) is strongly indicative of H-bonding.

The small shift of $\tilde{\nu}$(H–C(2)) implies weak H-bonding, which could be easily destroyed by dissolving the compound in a molecular (neutral) solvent. Nevertheless, the spectra of the CD$_2$Cl$_2$ solution of **6** in the $\tilde{\nu}$(CH) region remain essentially unchanged, except that the $\tilde{\nu}$(H–C(2)) band becomes a doublet (*Fig. 4*). The spectra (*Fig. 4*) do not exhibit any other spectral markers of isolated cations or anions (*Tables 4* and *5*), *i.e.*, ion pairing is not destroyed by the solvent. Probably, the EMIM$^+$ and BF$_4^-$ ions are held together mainly by powerful *Coulomb* attractions, and H-bonding plays

Table 3. *IR Spectra of* **6**

Exper. IR (liq.)	Exper. *Raman* (liq.)		Computations (B3LYP/6-31G*)				
$\tilde{\nu}$ [cm^{-1}]	$\tilde{\nu}$ [cm^{-1}]	ρ[a])	$\tilde{\nu}$ [cm^{-1}][b])	I_{IR} [km/mol]	I_{Ra} [Å^4/amu]	ρ	Assignment[c])
3166*s*	3172*w*	0.63	3178	1	100	0.13	ν(H−C(4)), ν(H−C(5)) (in-phase)
			3161	4	51	0.80	ν(H−C(4)), ν(H−C(5)) (out-of-phase)
3125*s-m*	3122*vw*	dp	3135	244	46	0.29	ν(H−C(2))
2989*m-w*			3007	14	41	0.83	ν_{as}(CH$_3$) (Me)
			2995	0	14	0.55	ν_{as}(CH$_3$), ν(CH$_2$)
ca. 2970*w* (sh)	2971*m*	0.42	2984	1	54	0.70	ν_{as}(CH$_3$), ν(CH$_2$)
			2982	9	75	0.82	ν_{as}(CH$_3$) (Me)
2952*w*	2946*m*	0.5	2949	22	96	0.60	ν_{as}(CH$_3$) (Et)
ca. 2917vv*w*			2913	32	117	0.21	ν_{s}(CH$_2$)
2892v*w*	2887*w*		2905	36	152	0.07	ν_{s}(CH$_3$) (Me)
			2885	26	109	0.06	ν_{s}(CH$_3$) (Et)
1619 (sh)	1606v*w*						
1576*s*	1569*m*	dp	1583	17	4	0.41	ν(C=C)
			1571	51	2	0.69	ν_{as}(N(1)C(2)N(3)), r(H−C(2))
1462*m*			1475	5	7	0.75	δ_{as}(CH$_3$) (Et)
			1472	8	21	0.77	δ_{as}(CH$_3$) (Me)
1458*m*	1453*m*	dp	1465	12	15	0.71	δ_{as}(CH$_3$) (Me)
			1460	11	9	0.73	δ(CH$_2$)
			1448	2	29	0.71	δ_{as}(CH$_3$) (Et)
1432v*w*	1422*s*	0.28	1431	11	16	0.77	δ_{s}(CH$_3$)
			1424	4	28	0.24	δ(CH$_2$), ν(ring)
1392*w*	1389*w*		1396	12	3	0.51	δ_{s}(CH$_3$) (Et), w(CH$_2$)
			1384	2	9	0.15	ν_{as}(C(2)N(1)C(5)), δ_{s}(CH$_3$) (Et)
1358*vw*	1346 (sh)		1360	7	1	0.74	w(CH$_2$)
1337*w*	1334*s*	0.47	1315	10	24	0.34	ν(Et−N), ν(Me−N), breathing
ca. 1300*w* (sh)	1296*w*		1293	2	2	0.63	r(H−C(4)), (H−C(5)), t(CH$_2$)
1286*m*			1259	473	0	0.45	ν(BF(5))
1250vv*w*			1256	8	3	0.67	r(H−C(2))
1172*s*	1170*w*	dp	1157	173	2	0.71	ν(Et−N), ν(Me−N)
			1144	26	4	0.54	r(CH$_3$)
			1133	4	2	0.25	r(CH$_2$), r(CH$_3$) (Et)
			1103	17	4	0.33	r(CH$_3$)
	1088*s*	0.44	1092	6	4	0.53	r(C−H)
			1088	11	6	0.38	r(CH$_3$)
1062vv*s* (br.)			1070	207	1	0.83	ν(BF(3)), ν(BF(2))
1038 (sh)			1041	41	2	0.69	δ(ring)
	1026*s*	0.45	1019	32	8	0.17	breathing, ν(Et−N), ν(Me−N)
			997	83	2	0.22	ν(BF(4)), ν(BF(2))
960v*w*	961*m*	0.55	985	181	1	0.82	γ(H−C(2))
912v*w*	914*m*	dp	939	3	6	0.33	ν(CC) (Et)
896*w*							
	861*w*	dp					
849*m*	829*s*	dp	811	0	0	0.81	γ(CH)
805*w*	804v*w*	dp	804	12	0	0.53	r(CH$_2$), r(CH$_3$) (Et)
758*m*	765v*s*	0.13	758	10	3	0.03	ν_{s}(BF$_4$)
			722	28	2	0.85	γ(H−C(4)), γ(H−C(5))
702*w*	701*m*	0.88	692	12	2	0.72	ν(Me−N), ν(Et−N)
649*m*	649v*w*	0.74	671	37	0	0.69	γ(Et−N), γ(H−C(2))
623*m*	624*w*	dp	627	3	1	0.73	γ(Me−N), ring-puckering
598*w*	599v*s*	0.39	589	1	6	0.25	ν(Et−N), ν(Me−N)

Table 3 (cont.)

Exper. IR (liq.)	Exper. *Raman* (liq.)		Computations (B3LYP/6-31G*)				
$\tilde{\nu}$ [cm^{-1}]	$\tilde{\nu}$ [cm^{-1}]	ρ[a])	$\tilde{\nu}$ [cm^{-1}][b])	I_{IR} [km/mol]	I_{Ra} [Å^4/amu]	ρ	Assignment[c])
521*w*	520*m*	dp	525	21	1	0.83	$\delta(\mathrm{BF_4})$
			515	3	0	0.47	$\delta(\mathrm{BF_4})$, $\nu(\mathrm{BF})$
	475*w*		511	2	0	0.86	$\delta(\mathrm{BF_4})$, $\nu(\mathrm{BF})$
423v*w*	438*m*	0.75	437	2	1	0.33	r(Et–N), r(Me–N)
404v*w*							
381v*w* (sh)			387	2	1	0.46	δ(NEt)
354v*w*	351*m*	dp	357	0	0	0.84	$\delta(\mathrm{BF_4})$
			352	0	0	0.80	$\delta(\mathrm{BF_4})$
294v*w*	286v*w*	dp	304	1	0	0.73	tors($\mathrm{CH_3}$) (Et)
243v*w*	241*m*	dp	242	2	1	0.86	γ(Me–N), ring puckering

[a]) Depolarization ratio; dp, depolarized. [b]) SQM Wavenumbers. [c]) ν, stretch; δ, bend; w, wagging; t, twisting; r, rocking; γ, out-of-plane; s, symmetric; as, antisymmetric.

Table 4. *SQM* (B3LYP/6-31G*) *Spectra of EMIM*$^+$

$\tilde{\nu}$ [cm^{-1}][a])	I_{IR} [km/mol]	Assignment[b])	$\tilde{\nu}$ [cm^{-1}][a])	I_{IR} [km/mol]	Assignment[b])
3178	8	ν(H–C(4)), (H–C(5)) (in-phase)	1311	11	ν(Et–N), (Me–N), breathing
3168	27	ν(H–C(4)), (H–C(5))	1288	0	r(H–C(4)), r(H–C(5)), t($\mathrm{CH_2}$)
		(out-of-phase)	1247	0	r(H–C(2))
3162	14	ν(H–C(2))	1153	10	ν(Et–N), ν(Me–N)
3012	0	$\nu_{\mathrm{as}}(\mathrm{CH_3})$ (Me)	1129	0	r($\mathrm{CH_3}$)
2998	0	$\nu_{\mathrm{as}}(\mathrm{CH_3})$, $\nu_{\mathrm{as}}(\mathrm{CH_2})$	1117	3	r($\mathrm{CH_2}$), r($\mathrm{CH_3}$) (Et)
2981	9	$\mathrm{v}_{\mathrm{as}}(\mathrm{CH_3})$, $\nu_{\mathrm{as}}(\mathrm{CH_2})$	1102	10	r($\mathrm{CH_3}$)
2973	6	$\nu_{\mathrm{as}}(\mathrm{CH_3})$ (Me)	1083	3	r(C–H)
2959	2	$\nu_{\mathrm{as}}(\mathrm{CH_3})$ (Et)	1077	4	r($\mathrm{CH_3}$)
2926	7	$\nu_{\mathrm{s}}(\mathrm{CH_2})$	1026	1	δ(ring)
2919	4	$\nu_{\mathrm{s}}(\mathrm{CH_3})$ (Me)	1015	0	breathing + ν(Et–N), ν(Me–N)
2897	4	$\nu_{\mathrm{s}}(\mathrm{CH_3})$ (Et)	937	3	ν(CC) (Et)
1582	35	ν(C=C)	851	0	γ(CH)
1572	52	ν_{as}(N(1)C(2)N(3)), r(H–C(2))	815	38	γ(H–C(2))
1464	7	$\delta_{\mathrm{as}}(\mathrm{CH_3})$ (Et)	787	2	r($\mathrm{CH_2}$), r($\mathrm{CH_3}$) (Et)
1462	15	$\delta_{\mathrm{as}}(\mathrm{CH_3})$ (Me)	734	20	γ(H–C(4)), γ(H–C(5))
1447	17	$\delta_{\mathrm{as}}(\mathrm{CH_3})$ (Me)	687	10	ν(Me–N), ν(Et–N)
1444	9	$\delta(\mathrm{CH_2})$	649	15	γ(Et–N), γ(H–C(2))
1435	16	$\delta_{\mathrm{as}}(\mathrm{CH_3})$ (Et)	620	8	γ(Me–N), ring puckering
1423	9	$\delta_{\mathrm{s}}(\mathrm{CH_3})$	580	2	ν(Et–N), ν(Me–N)
1409	5	$\delta(\mathrm{CH_2})$, ν(ring)	425	0	r(Et–N), r(Me–N)
1394	5	$\delta_{\mathrm{s}}(\mathrm{CH_3})$ (Et), w($\mathrm{CH_2}$)	375	0	δ(EtN)
1379	4	ν_{as}(C(2)N(1)C(5)), $\delta_{\mathrm{s}}(\mathrm{CH_3})$ (Et)	286	0	tors($\mathrm{CH_3}$) (Et)
1361	15	w($\mathrm{CH_2}$)	229	2	γ(Me–N), ring puckering

[a]) SQM Wavenumbers. [b]) ν, stretch, δ, bend; w, wagging; t, twisting; r, rocking; γ, out-of-plane; s, symmetric; as, antisymmetric.

only a minor role. The latter is obvious from consideration of the computed energy of the ion-pair formation in vacuum, which is equal to 97 kcal/mol at the B3LYP/6-31G* level.

Table 5. *SQM Vibrational Spectra of* BF_4^-

$\tilde{\nu}$ [cm^{-1}]^{a})	I_{IR} [km/mol]	Assignment^{b})	$\tilde{\nu}$ [cm^{-1}]^{a})	I_{IR} [km/mol]	Assignment^{b})
1145	347	$\nu_{as}(BF_4)$	519	3	$\delta(BF_4)$
1143	347	$\nu_{as}(BF_4)$	519	3	$\delta(BF_4)$
1142	347	$\nu_{as}(BF_4)$	350	0	$\delta(BF_4)$
762	0	$\nu_{s}(BF_4)$	350	0	$\delta(BF_4)$
520	3	$\delta(BF_4)$			

a) SQM Wavenumbers. b) ν, stretch; δ, bend; s, symmetric; as, asymmetric.

Concluding Remarks. – We have demonstrated that SQM successfully reproduces the spectra of $[EMIM][BF_4]$ (**6**). The computations reveal that normal modes of the $EMIM^+ \cdot BF_4^-$ ion pair rather closely resemble those of the isolated ions $EMIM^+$ and BF_4^-, except for antisymmetric BF stretching vibrations of the anion, and out-of-plane and stretching vibrations of the H–C(2) moiety of the cation. The most plausible explanation of the pronounced changes of the latter vibrations upon formation of the ion pair is H-bonding between the H–C(2) proton on the cation and the BF_4^- anion. These weak H-bonds are of minor importance when compared with powerful *Coulomb* interactions between the ions that keeps them closely associated even in dilute CD_2Cl_2 solutions. According to the 'gas-phase' computations, in these associates, the BF_4^- anion is positioned over the imidazolium ring of the $EMIM^+$ cation and has short contacts not only with H–C(2) but also with a proton of the Me–N(3) group.

The financial support of the quantum-chemical computations by the *Russian Foundation for Basic Research* (Grant 03-07-90092) is gratefully acknowledged. The authors are also indebted to all staff members of the Computational Alpha-Cluster of the *Kazan Scientific Center of the Russian Academy of Sciences* and especially to Dr. *G. A. Shamov* for technical assistance in the computations and valuable advice. Special thanks are due to Dr. *M. A. Tafipolsky* for permission to use his version of the program, adopted from *Sipachev* [14].

REFERENCES

[1] 'Ionic Liquids in Synthesis' Eds. P. Wasserscheid and T. Welton, Wiley-VCH Verlag GmbH&Co., Weinheim, 2002.

[2] C. M. Dymek Jr., D. A. Grossie, A. V. Fratini, W. W. Adams, *J. Mol. Struct.* **1989**, *213*, 25.

[3] K. M. Dieter, C. M. Dymek Jr., N. E. Heimer, J. W. Rowang, J. S. Wilkes, *J. Am. Chem. Soc.* **1988**, *110*, 2722.

[4] A. Elaiwi, P. B. Hitchcock, K. R. Seddon, N. Srinivasan, Y.-M. Tan, T. Welton, J. A. Zora, *J. Chem. Soc., Dalton Trans.* **1995**, 3467.

[5] E. A. Turner, C. C. Pye, R. D. Singer, *J. Phys. Chem. A* **2003**, *107*, 2277.

[6] C. G. Hanke, S. L. Price, R. M. Linden-Bell, *Mol. Phys.* **2001**, *99*, 801.

[7] P. A.Z. Suarez, S. Einloft, J. E.L. Dullius, R. F. de Souza, J. Dupont, *J. Chim. Phys.* **1998**, *95*, 1626.

[8] N. Kuhn, M. Walker, M. Steimann, *Z. Naturforsch. B* **2002**, *57*, 248.

[9] R. G. Parr, W. Yang, 'Density Functional Methods of Atoms and Molecules', Oxford University Press, New York, 1989.

[10] K. R. Seddon, A. Stark, M.-J. Torres, *Pure Appl. Chem.* **2000**, *72*, 2275.

[11] M. J. Frisch, G. W. Trucks, H. B. Schlegel, G. E. Scuseria, M. A. Robb, J. R. Cheeseman, V. G. Zakrzewski, J. A. Montgomery, R. E. Stratmann, J. C. Burant, S. Dapprich, J. M. Millam, A. D. Daniels, K. N. Kudin, M. C. Strain, O. Farkas, J. Tomasi, V. Barone, M. Cossi, R. Cammi, B. Mennucci, C. Pomelli, C. Adamo, S. Clifford, J. Ochterski, G. A. Petersson, P. Y. Ayala, Q. Cui, K. Morokuma, D. K. Malick, A. D. Rabuck, K. Raghavachari, J. B. Foresman, J. Cioslowski, J. V. Ortiz, B. B. Stefanov, G. Liu, A. Liashenko, P. Piskorz, I. Komaromi, R. Gomperts, R. L. Martin, D. J. Fox, T. Keith, M. A. Al-Laham, C. Y. Peng, A. Nanayakkara, C. Gonzalez, M. Challacombe, P. M. W. Gill, B. G. Johnson, W. Chen, M. W. Wong, J. L. Andres, M. Head-

Gordon, E. S. Replogle, J. A. Pople, 'Gaussian 98 (Revision A.2)', Gaussian, Inc., Pittsburgh, Pa., USA, 1998.
[12] A. D. Becke, *J. Chem. Phys.* **1993**, *98*, 5648.
[13] A. D. Becke, *Phys. Rev. A* **1988**, *38*, 3098.
[14] V. A. Sipachev, *J. Mol. Struct.* **2001**, *567–568*, 67; V. A. Sipachev, *Struct. Chem.* **2000**, *2/3*, 167.
[15] G. Rauhut, P. Pulay, *J. Phys. Chem.* **1995**, *99*, 3093; G. Rauhut, P. Pulay, *J. Am. Chem. Soc.* **1995**, *117*, 4167.
[16] J. Baker, A. Jarzecki, P. Pulay, *J. Phys. Chem. A* **1998**, *102*, 1412.
[17] S. A. Katsyuba, J. Grunenberg, R. Schmutzler, *J. Mol. Struct*. **2001**, *559*, 315.
[18] S. A. Katsyuba, E. E. Vandyukova, *Chem. Phys. Lett.* **2003**, *377*, 658.
[19] J. Fuller, R. T. Carlin, H. C. De Long, D. Haworth, *J. Chem. Soc., Chem. Commun*. **1994**, 299.
[20] Z. Meng, A. Dölle, W. R. Carper, *J. Mol. Structure (Theochem)* **2002**, *585*, 119.
[21] T. I. Morrow, E. J. Maginn, *J. Phys. Chem., B* **2002**, *106*, 12807.
[22] A. V. Iogansen, *Spectrochim. Acta Part A* **1999**, *55*, 1585.

Received June 16, 2004